Sensors and Materials, Vol. 35, No. 12 (2023) 4049–4059
MYU Tokyo

S & M 3467

Microwave Dielectric Properties of Sn-substituted $Nd(Ti_{0.5}Mo_{0.5})O_4$ Ceramics for Use in Patch Antenna Liquid Sensor

Yih-Chien Chen* and Tse-Lung Lin

Department of Electrical Engineering, Lunghwa University of Science and Technology,
No. 300, Sec. 1, Wanshou Rd., Guishan District, Taoyuan City 333326, Taiwan

(Received July 14, 2023; accepted December 8, 2023)

Keywords: liquid sensor, patch antenna, microwave dielectric properties

The microwave dielectric characteristics of $NdTi_{(0.5-x)}Sn_xMo_{0.5}O_4$ were examined using densification and X-ray diffraction (XRD) patterns. The volume of the unit cell increased as x increased from 0 to 0.05. The $Nd(Ti_{0.49}Sn_{0.01}Mo_{0.5})O_4$ ceramics sintered at 1425 °C for 4 h achieved a maximum relative density of 98.9%. The $Nd(Ti_{0.49}Sn_{0.01}Mo_{0.5})O_4$ ceramics had a dielectric constant (ε_r) of 18.2 and an unloaded quality factor ($Q_u \times f$) of 35700 GHz (at 17.6 GHz) after being sintered at 1425 °C for 4 h, with a resonance frequency temperature coefficient (τ_f) of −31.2 ppm/°C. The patch antenna liquid sensor development processes and testing results were given. The observed resonance frequencies in water and acetone were 1.66 and 2.53 GHz, respectively.

1. Introduction

These days, many industrial production facilities incorporate environmental sensor monitoring to ensure safety. Monitoring can be achieved with the utilization of the material characterization of liquid. Different techniques for material characterization based on microwave technology have been developed. There are various microwave-based liquid sensors, including those used in resonant and nonresonant methods.(1) In comparison with the sensor used in the nonresonant method, a resonance-based liquid sensor is good for better precision and sensitivity. A planar microstrip resonator is a type of resonance-based liquid sensor, suitable for the current era owing to its easy design. More specifically, in harsh environment operations, a patch antenna liquid sensor on ceramic is highly desirable, owing to its solid and high-quality-factor features.

An optimized dielectric constant, a high quality factor, and a small temperature coefficient of resonance frequency are the three microwave dielectric properties of materials that must be taken into consideration when designing patch antenna liquid sensors. An application patch antenna for wireless high-temperature sensors using a $(Mg_{0.93}Zn_{0.07})_2SnO_4$ ceramic substrate was developed.(2) The dielectric constant of the ceramic substrate is affected by the temperature coefficient of resonance frequency. When temperature changes, the dielectric constant of the

*Corresponding author: e-mail: ee049@mail.lhu.edu.tw
https://doi.org/10.18494/SAM4585

ISSN 0914-4935

substrate will change and affect the performance of patch antenna sensors. Small devices with a high dielectric constant can be manufactured. On the other hand, the high dielectric constant of the substrate will affect the performances of patch antenna sensors because of the effective dielectric constants that correspond to the substrate and liquid under testing. For usage in patch antenna liquid sensors, moderate-dielectric-constant materials are being developed to replace high-dielectric-constant materials. The patch antenna losses are represented by the quality factor. Typically, losses in antennas have several forms, such as radiation, conduction, and dielectric.[3] As a result, all of these losses have an impact on the total quality factor. Conduction and dielectric losses reduce the patch antenna liquid sensor efficiency.[4] Patch antenna efficiency, on the other hand, is enhanced by lesser radiation loss. All of these losses affect the read range and bandwidth of the patch antenna temperature sensor. A small temperature coefficient of resonance frequency is needed to minimize environmental inferences.

Rare-earth niobate ($RENbO_4$) ceramics were synthesized using a typical solid-state reaction for prospective use in resonators, filters, and antennas in current communication systems.[5] When the $LaNbO_4$ and $NdNbO_4$ ceramics were sintered at 1250 °C for 4 h, they produced dielectric constants (ε_r) of 19.3 and 19.6, unloaded quality factors ($Q_u \times f$) of 54,400 and 33,000 GHz, and temperature coefficients of resonance frequency (TCF) of 9 and −24 ppm/°C, respectively.[6] The application patch antenna for 5G mobile communication in the FR2 band using the $Nd(Ti_{0.5}Mo_{0.5})O_4$ ceramic substrate was developed.[7] The ceramic substrate of $Nd(Ti_{0.5}Mo_{0.5})O_4$ has good performance in the patch antenna substrate. The microwave dielectric properties of $Nd(Ti_{0.5}Mo_{0.5})O_4$ can be implemented to the patch antenna because the ionic radii of Ti^{4+} and Mo^{6+} ions are comparable to that of Nb^{5+} ions (0.064 nm),[8] and Nb^{5+} ions could be substituted by Ti^{4+} and Mo^{6+} ions to generate $Nd(Ti_{0.5}Mo_{0.5})O_4$. Furthermore, the ion polarizabilities of Ti^{4+} and Mo^{6+} are lower than those of Nb^{5+}, and as a result, permittivity decreases.[9] Consequently, there is reduced cross-coupling and transmission attenuation. Considering that the ionic radius of Sn^{4+} ions (0.0694 nm) is comparable to that of Ti^{4+} ions (0.0605 nm), the investigation into how the substitution of Ti^{4+} by Sn^{4+} to form $NdTi_{(0.5-x)}Sn_xMo_{0.5}O_4$ ceramics was encouraged.[8] They were discovered to have a great deal of potential for use in patch antenna liquid sensors. However, there was no specific data in the literature related to their application in patch antenna liquid sensors. The impacts of the amount of Sn substitution and sintering temperature on the microwave dielectric properties of $NdTi_{(0.5-x)}Sn_xMo_{0.5}O_4$ ceramics was examined in this work. Densification and X-ray diffraction (XRD) patterns were used to examine these various microwave dielectric properties.

Microwave-based liquid sensors are classified into two categories: those for reflection-based methods and those for transmission-based methods. Two types of microwave-based liquid sensor have been developed. The microstrip monopole antenna liquid sensor with an asymmetric coplanar strip-based feeding line has been developed for liquid permittivity measurements using reflection-based methods. The dielectric constant measurement range is 20–80 for the liquid under testing.[10] The transmission line loaded with two rectangular split-ring resonators has been developed for solid and liquid permittivity measurements using transmission-based methods. The dielectric constant measurement range is 2–23 for the liquid under testing.[11] Patch antennas are used in many commercial applications such as mobile radio and wireless

communications because they are fairly small, efficient, and simple to manufacture. A standard patch antenna using a commercial substrate has a rectangular half-wavelength form.[12] However, its chemical stability is low; thus, it cannot be used in a corrosive environment. To avoid the corrosion of the liquid sample on the antenna, the antenna has a ceramic substrate structure in this study. A patch antenna liquid sensor for concentration determination was developed and demonstrated by combining the advantages of a low-profile patch antenna with the use of microwave ceramic with a moderate dielectric constant as a substrate. The suggested patch antenna liquid sensor was simple to manufacture owing to its single dielectric substrate without any via or through holes.

2. Materials and Methods

The chemicals used are the high-purity raw materials Nd_2O_3 (99.9%), TiO_2 (99.0%), and MoO_3 (99.9%) powders. The compound that was prepared is $NdTi_{(0.5-x)}Sn_xMo_{0.5}O_4$. The samples were made using the traditional mixed-oxide technique. A stoichiometric ratio was used to measure the substance's raw materials, which were subjected to ball milling in alcohol, drying, and subsequent calcining in air for 4 h at 1200 °C. The calcined powder should be regrounded with the PVA solution acting as a binder. Following that, the powder was finely ground and sieved using a 200-mesh sieve. Then the obtained powder was axially compressed into pellets measuring 11 mm in diameter and 6 mm in thickness with a pressure of 2000 kg/cm^2 applied to the sample. Subsequently, these pellets were subjected to sintering in the presence of air for 4 h at temperatures ranging from 1375 to 1450 ℃. For both the cooling and heating processes, a rate of 10 ℃/min was selected.

The phases of the sample were analyzed after sintering with a Rigaku D/MAX-2200 X-ray Diffraction Meter equipped with CuKα radiation (at 30 kV and 20 mA). The scanning range for 2θ was adjusted between 20° and 60°. To identify the material's composition, the X-ray diffraction data obtained was compared with the JCPDS database entries. The Archimedes method, utilizing distilled water as the liquid, was employed to calculate the apparent densities of the samples. Subsequently, the relative density (RD) was calculated by comparing the apparent and theoretical densities.

The microwave dielectric properties of the specimens were evaluated using the post-resonator method developed by Hakki and Coleman.[13] In this method, the specimens were prepared in the form of cylindrical shapes with length L and diameter D. The specimens' aspect ratio (D/L) was about 1.6, falling within the range specified by Kobayashi and Katoh.[14] To measure the microwave properties, the cylindrical specimens were placed between two parallel metal plates, forming a transmission-type resonator. To ensure effective transmission and reception of microwave signals, two compact antennas were strategically positioned near the specimen, facilitating efficient coupling with the resonator. The coaxial transmission line's front-end antenna served as the input for the signal, while the other-end antenna coupled the electromagnetic wave that satisfied the resonator conditions. The antennas were connected to an Agilent N5230A network analyzer.

The resonance characteristics of the system were dependent on the size and dielectric properties of the specimen. Electric-field probes were used to couple the microwave energy. The

TE_{011} resonant method was specifically employed to determine the specimen's loss factor and dielectric constant. The TE_{011} resonant method was identified using the mode identification method developed by Wheless and Kajfez.[15] The Agilent N5230A network analyzer was utilized to determine the TE_{011} resonance frequency of the dielectric resonator, from which the dielectric constant and quality factor were calculated. The measurement procedure for determining the temperature coefficient of resonance frequency (τ_f) was conducted in a similar manner to that used to measure the dielectric constant. The experimental setup involved placing the test cavity inside a temperature-controlled chamber and gradually increasing the temperature from 25 to 75 ℃. For each 10 ℃, the resonance frequency was measured, and the temperature coefficient of resonance frequency (τ_f) was calculated using the provided formula, giving the value in parts per million per degree Celsius (ppm/℃).

$$\tau_f = \frac{f_2 - f_1}{f_1(T_2 - T_1)} \tag{1}$$

Here, the resonance frequencies at temperatures T_1 and T_2 are denoted by f_1 and f_2, respectively.

The patch antenna sensor was examined by analyzing its transmission line model. A commercially available electromagnetic simulator was utilized for simulation purposes. The design process commenced by considering a rectangular patch with a resonance frequency of 3.5 GHz. The nonradiating edges were changed to be half the guided wavelength at a frequency of 3.5 GHz to create an early design for the patch antenna.[16] The ceramic substrate was polished using a grinder to achieve the desired dimensions. Subsequently, both sides of the substrate were polished using water sandpaper. Then cleaning was carried out, involving a 40 min treatment with acetone and an ultrasonic vibration cleaning machine. The acetone was used to clean the remaining material that adhered to it during the polishing process. Subsequently, the ceramic substrate was thoroughly rinsed with deionized water to remove any residual particles or impurities. The substrate was carefully dried by placing it inside a controlled environment, such as a box with heated air circulation, ensuring efficient moisture removal. Silver glue was applied to the substrate using a printer, and then the substrate was dried at 150 ℃ for 1 h in a hot air circulation box. Laser ablation with a laser engraving machine was performed to complete the fabrication of the microwave microstrip patch antenna. For the measurement of return loss, a PNA-L network analyzer (N5230A) was used. A coaxial connector was soldered to the microstrip feed line, enabling signal output from the coplanar patch antenna to Port 1 of the PNA-L network analyzer.

3. Results and Discussion

Figure 1 shows the X-ray diffraction patterns of $Nd(Ti_{0.49}Sn_{0.01}Mo_{0.5})O_4$ at 1375–1450 ℃ for 4 h. The $Nd(Ti_{0.5}Mo_{0.5})O_4$ phase exhibits a tetragonal crystal structure. (ICDD-PDF 49-0554) belongs to the l41/a(88) space group. In addition to the primary phase $Nd(Ti_{0.5}Mo_{0.5})O_4$, a secondary phase of $Nd_2Ti_2O_7$ was observed, represented by a solid circle, compared with the ICDD-PDF 49-0554 reference. The primary phase keeps a reasonably stable composition over

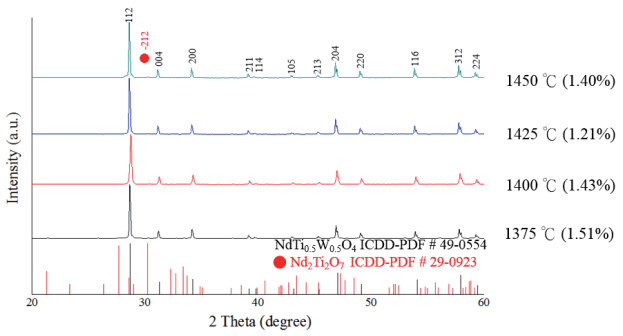

Fig. 1. (Color online) X-ray diffraction patterns of $Nd(Ti_{0.49}Sn_{0.01}Mo_{0.5})O_4$ ceramics with different sintering temperatures for 4 h.

sintering temperatures, although the secondary phase persists. The secondary-phase $Nd_2Ti_2O_7$ occurred perhaps because the sintering temperature is too high, causing the evaporation of molybdenum trioxide and the formation of $Nd_2Ti_2O_7$. The characteristics of the $Nd(Ti_{0.49}Sn_{0.01}Mo_{0.5})O_4$'s microwave dielectric can be affected by the existence of the secondary phase. $Nd_2Ti_2O_7$ ceramics exhibit a relative dielectric constant (ε_r) of 36, a quality factor times resonance frequency ($Q_u \times f$) of 16,400 GHz, and a temperature coefficient of frequency (TCF) of −118 ppm/°C.[17] Compared with $Nd(Ti_{0.49}Sn_{0.01}Mo_{0.5})O_4$ ceramics, $Nd_2Ti_2O_7$ ceramics have a greater ε_r value. However, compared with $Nd(Ti_{0.49}Sn_{0.01}Mo_{0.5})O_4$, $Nd_2Ti_2O_7$ ceramics with the $Nd_2Ti_2O_7$ phase showed lower $Q_u \times f$ values and a larger negative TCF. This indicates that the formation of the $Nd_2Ti_2O_7$ phase contributed to the decrease in ($Q_u \times f$) and the shift towards a more negative TCF in the sample. $Nd_2Ti_2O_7$ ceramics exhibit a higher relative dielectric constant (ε_r) compared with $Nd(Ti_{0.49}Sn_{0.01}Mo_{0.5})O_4$ ceramics. However, in terms of $Q_u \times f$ and TCF, $Nd_2Ti_2O_7$ ceramics exhibit lower $Q_u \times f$ values and a larger negative TCF. This indicates that the presence of the $Nd_2Ti_2O_7$ phase has a detrimental effect on $Q_u \times f$ and results in a negative TCF for the sample.

The unit cell volumes of $NdTi_{(0.5-x)}Sn_xMo_{0.5}O_4$ ceramics increased from 315.3928 to 315.5922 as the value of x increased from 0 to 0.05. This can be attributed to the fact that the ionic radius of Sn^{4+} ions (0.0694 nm) is larger than that of Ti^{4+} ions (0.0605 nm).[8] The intensities of the (1 1 2) diffraction peak of $Nd(Ti_{0.49}Sn_{0.01}Mo_{0.5})O_4$ and the (2 1 1) diffraction peak of $Nd_2Ti_2O_7$ were utilized in the calculation to determine the quantity of the secondary-phase $Nd_2Ti_2O_7$. The formula for the calculation is

$$NdTi_{0.5}Mo_{0.5}O_4\ (\text{vol}\%) = \frac{I_{A(1\,1\,2)}}{I_{A(1\,1\,2)} + I_{B(2\,1\,1)}} \times 100, \tag{2}$$

where I_A represents the highest intensity of the diffraction line from $Nd(Ti_{0.49}Sn_{0.01}Mo_{0.5})O_4$ (1 1 2), and I_B represents the highest intensity of the diffraction line from $Nd_2Ti_2O_7$ (2 1 1). The presence of the second phase in $Nd(Ti_{0.49}Ti_{0.01}Mo_{0.5})O_4$, which was sintered for 4 h from 1375 to 1450 °C, varied from 1.21% to 1.51%. The presence of the second phase in $NdTi_{(0.5-x)}Sn_xMo_{0.5}O_4$,

which was sintered for 4 h at 1425 °C, varied from 1.21% to 1.31% as the value of x ranged from 0 to 0.05. The presence of the second phase, which remained relatively stable across different sintering temperatures and amounts of Sn^{4+} substitution, shows that the second phase has little impact on the specimen's microwave dielectric characteristics.

In Figs. 2 and 3, the relative density and ε_r of the $NdTi_{(0.5-x)}Sn_xMo_{0.5}O_4$ ceramics are shown for sintering temperatures of 1375–1450 °C for 4 h. The highest relative density is achieved at 1425 °C, with a subsequent decrease observed beyond this temperature. At a sintering temperature of 1425 °C for 4 h, the $Nd(Ti_{0.49}Sn_{0.01}Mo_{0.5})O_4$ ceramics achieved a maximum relative density of 98.9%. As the sintering temperature increased from 1375 to 1425 °C, the relative dielectric constant (ε_r) also increased from 15.7 to 18.2. Increasing the sintering temperature from 1425 to 1450 °C for 4 h caused the relative dielectric constant (ε_r) to decrease from 18.2 to 17.3. This change in ε_r follows a similar pattern to the relative density, indicating that a higher relative density corresponds to a higher ε_r owing to reduced porosity. In the case of $NdTi_{(0.5-x)}Sn_xMo_{0.5}O_4$ ceramics sintered at 1425 °C, an increase in x from 0 to 0.05 resulted in a decrease in ε_r from 18.5 to 16.7. Many different factors affect the relative dielectric constant (ε_r), which can be classified as intrinsic and extrinsic factors.[18,19] Intrinsic factors, such as ionic polarizability, and extrinsic factors, including relative density, external porosity, and the presence of secondary phases, can influence the relative dielectric constant (ε_r). The dielectric constant (ε_r) of the $NdTi_{(0.5-x)}Sn_xMo_{0.5}O_4$ ceramic can be determined using the Clausius–Mossotti equation. The ε_r calculated through this equation represents an intrinsic factor contributing to the dielectric properties. It is influenced by the molar volume and ionic polarization of the material. According to the Clausius–Mossotti equation, a smaller molar volume or a larger ionic polarization corresponds to a higher relative dielectric constant (ε_r). Among these factors, ionic polarization has a significantly greater impact on ε_r than the molar volume. In this study, the relative dielectric constant (ε_r) of the $NdTi_{(0.5-x)}Sn_xMo_{0.5}O_4$ ceramic is influenced by the molar volume and ionic polarizability. The unit cell volumes of the $NdTi_{(0.5-x)}Sn_xMo_{0.5}O_4$ ceramics increased from 315.3928 to 315.5922 Å^3 as x increased from 0 to 0.05. The

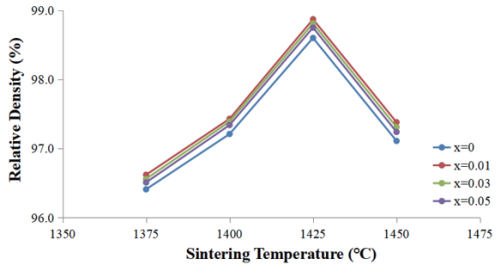

Fig. 2. (Color online) Relative densities of $NdTi_{(0.5-x)}Sn_xMo_{0.5}O_4$ ceramics with different sintering temperatures for 4 h.

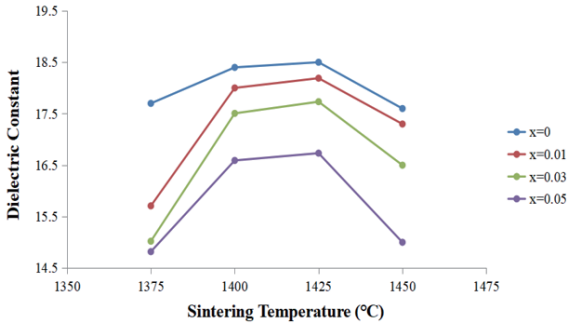

Fig. 3. (Color online) Dielectric constants of $NdTi_{(0.5-x)}Sn_xMo_{0.5}O_4$ ceramics with different sintering temperatures for 4 h.

ionic polarizations of Ti^{4+} and Sn^{4+} ions are 2.93 and 2.83 Å³, respectively. As x increases, the sum of the ionic polarizations of the individual ions in the $NdTi_{(0.5-x)}Sn_xMo_{0.5}O_4$ ceramics decreases. Therefore, it can be inferred that the relative dielectric constant (ε_r) of the $NdTi_{(0.5-x)}Sn_xMo_{0.5}O_4$ ceramics decreases with increasing x.

Figures 4 and 5 present the values of $Q_u \times f$ and TCF for the $NdTi_{(0.5-x)}Sn_xMo_{0.5}O_4$ ceramics following sintering at temperatures ranging from 1375 to 1450 °C for a duration of 4 h. Among these ceramics, the $Nd(Ti_{0.49}Sn_{0.01}Mo_{0.5})O_4$ specimens, sintered at 1425 °C for 4 h, demonstrated the highest $Q_u \times f$ value of 35,700 GHz. Microwave dielectric loss is influenced by various factors, encompassing both intrinsic and extrinsic losses. Intrinsic loss pertains to the lattice vibrational modes inherent to the material. Extrinsic loss, in the context of microwave dielectric properties, is attributable to external factors that affect the performance of the material. These factors include parameters such as density, porosity, presence of secondary phases, impurities, oxygen vacancies, grain size, and lattice defects. Understanding and controlling these extrinsic factors are crucial for optimizing the dielectric properties of materials used in microwave applications.[20,21] The $Q_u \times f$ values of $NdTi_{(0.5-x)}Sn_xMo_{0.5}O_4$ ceramics show a tendency to increase as x increases, suggesting that densification plays a significant role in controlling the $Q_u \times f$ values under strain. Notably, among the ceramics in the series, $Nd(Ti_{0.49}Sn_{0.01}Mo_{0.5})O_4$ ceramics demonstrate the highest relative density, reaching a maximum of 98.87%. This indicates that the densification process has a direct impact on the $Q_u \times f$ values, highlighting the importance of achieving high relative density for improved microwave performance. The composition and amount of the second phase in ceramics will affect the TCF. On the other hand, the steady composition of the $NdTi_{(0.5-x)}Sn_xMo_{0.5}O_4$ ceramics results in no significant change in the TCF across the studied range of sintering temperatures. This suggests that the TCF is not significantly influenced by the sintering temperature when the composition remains constant. The TCF values of $Nd(Ti_{0.49}Sn_{0.01}Mo_{0.5})O_4$ ceramics varied between −26.5 and −31.2 ppm/°C depending on the sintering conditions. TCF of −31.2 ppm/°C was observed in the $Nd(Ti_{0.49}Ti_{0.01}Mo_{0.5})O_4$ ceramic, which was sintered at 1425 °C for 4 h.

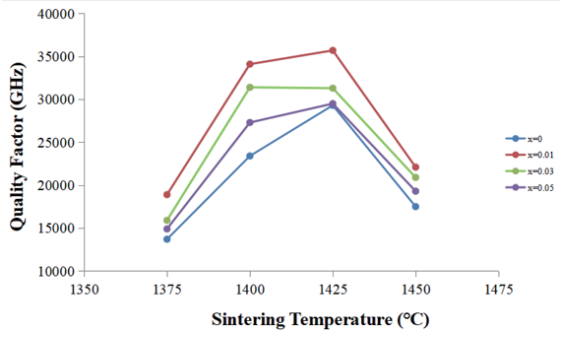

Fig. 4. (Color online) Quality factors of $NdTi_{(0.5-x)}Sn_xMo_{0.5}O_4$ ceramics with different sintering temperatures for 4 h.

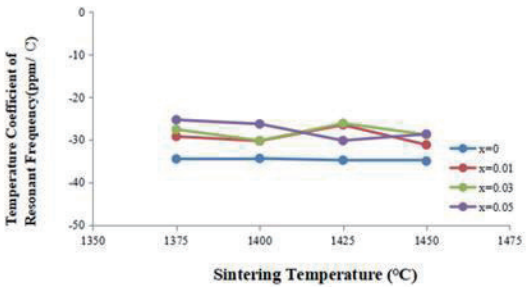

Fig. 5. (Color online) Temperature coefficients of the resonance frequency of $NdTi_{(0.5-x)}Sn_xMo_{0.5}O_4$ ceramics with different sintering temperatures for 4 h.

Figure 6 presents a detailed photography of a patch antenna installed on a substrate made of $Nd(Ti_{0.49}Ti_{0.01}Mo_{0.5})O_4$. The design includes a precisely engineered 50-ohm microstrip line that serves as the dedicated feed line for the patch antenna. The dimensions of the microstrip line are determined using specific closed-form formulas described in Ref. 22. These equations determine the dimensions by considering the thickness of the dielectric substance and the existence of an infinite ground plane, ensuring accurate calculations for optimal performance. To ensure accuracy and validity, the calculated dimensions are subsequently verified using AWR Microwave Office, a reliable software tool commonly employed in microwave design and simulation. The rectangular patch used in the design has specific dimensions of 9.7 mm × 13.0 mm. Figure 7 showcases the return losses exhibited by the patch antenna in an air environment. According to the simulation results, the return loss at a frequency of 3.44 GHz is −29.99 dB, while the measured return loss at the same frequency is −35.10 dB. Similarly, at a frequency of 3.47 GHz, the simulation predicts a return loss of −29.99 dB, while the measured return loss is −35.10 dB. These results indicate a close alignment between the measured resonance frequencies and the simulated resonance frequencies, indicating a good agreement between the two.

The return loss of the patch antenna liquid sensor with different concentrations of water in acetone is presented in Fig. 8. It can be observed that as the concentration of water in acetone increases, the resonance frequency of the sensor decreases. Indeed, the observed trend in the resonance frequency of the patch antenna liquid sensor aligns with the expected behavior based on the dielectric properties of the liquid. As the concentration of water in acetone varies, the

Fig. 6. (Color online) Patch antenna liquid sensor prototype on a $Nd(Ti_{0.49}Ti_{0.01}Mo_{0.5})O_4$ substrate.

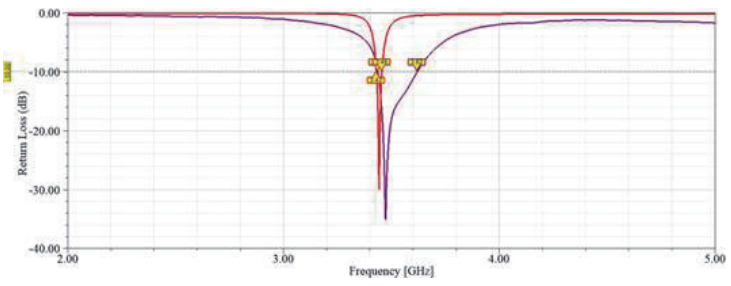

Fig. 7. (Color online) Measured return loss of the patch antenna liquid sensor in air.

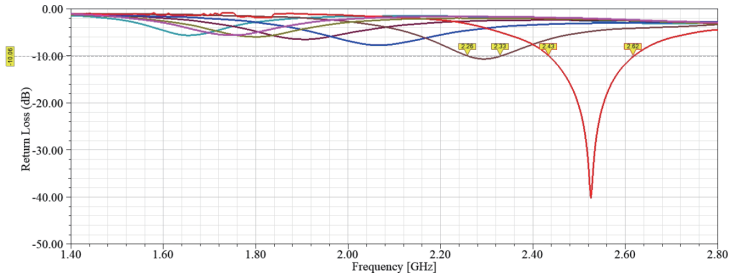

Fig. 8. (Color online) Variation in measured return loss for the patch antenna liquid sensor with the concentration of water in acetone.

permittivity of the liquid changes, leading to a corresponding shift in the resonance frequency of the sensor. This relationship confirms that the resonance frequency is influenced by the permittivity of the liquid, as anticipated.[10] The measurement results indicate that as the concentration of water in acetone increases from 0 to 100%, the resonance frequencies of the patch antenna liquid sensor consistently decrease. The relationship between the concentration of water and the resonance frequency appears to be linear, as the resonance frequencies decrease in a nearly linear fashion with increasing water concentration. As the concentration of water in acetone increases, the return loss of the patch antenna decreases. This is because the impedance matching between the antenna and the liquid changes, resulting in higher losses. According to the result, this manufactured patch antenna can be used as a sensor to determine the concentration of water in the acetone by monitoring the resonance frequency. This type of sensor is usually used in the chemical industry. As a future development, this sensor's dielectric constant should be determined for its more detailed characterization.

4. Conclusions

In this study, we examined the impacts of sintering temperature and duration on the dielectric properties of $Nd(Ti_{0.5}Mo_{0.5})O_4$ ceramics. The X-ray diffraction patterns of the $Nd(Ti_{0.49}Sn_{0.01}Mo_{0.5})O_4$ ceramics exhibited minimal variation across different sintering temperatures. However, it was observed that the dielectric properties of the ceramics were influenced by specific sintering conditions. The $Nd(Ti_{0.49}Sn_{0.01}Mo_{0.5})O_4$ ceramics, sintered at 1425 °C for 4 h had a relative density of 98.9%, ε_r of 17.7, $Q_u \times f$ of 35700 GHz, and a TCF of −31.2 ppm/°C. The structure of the patch antenna liquid sensor was designed to be simple and easy to manufacture. Its robustness, low loss, and high sensitivity make it highly appealing for further development and application in various industrial environments.

Acknowledgments

The authors would like to thank the Ministry of Science and Technology in Taiwan for financially supporting this research under Contract No. MOST 111-2221-E-262-001.

References

1 L. F. Chen, C. Ong, C. Neo, V. Varadan, and V. K. Varadan: Microwave Electronics: Measurement and Materials Characterization (John Wiley & Sons, Chichester, 2004). https://doi.org/10.1002/0470020466
2 Y. C. Chen, M. Z. Weng, Y. X. Du, and C. L. Hsiao: J. Mater. Sci.: Mater. Electron **29** (2018) 4717. https://doi.org/10.1007/s10854-017-8424-y
3 D. M. Pozar: Microwave Engineering (Wiley, New York, 2011) 4th ed.
4 W. L. Stutzman and G. A. Thiele: Antenna Theory and Design (John Wiley & Sons, Hoboken, 2012) 3rd ed.
5 G. J. McCarthy: Acta Crystallogr., Sect. B: Struct. Sci. **27** (1971) 2285. https://doi.org/10.1107/S0567740871005697
6 D. W. Kim, D. K. Kwon, S. H. Yoon, and K. S. Hong: J. Am. Ceram. Soc. **89** (2006) 3861. https://doi.org/10.1111/j.1551-2916.2006.01302.x
7 Y. T. Liao, Y. C. Chen, T. L. Lin, Y. C. You, and C. C. Kuo: Ferroelectr. **600** (2022) 203. https://doi.org/10.1080/00150193.2022.2115811
8 R. D. Shannon: Acta Crystallogr., Sect. A: Found. Crystallogr. **32** (1976) 751. https://doi.org/10.1107/S0567739476001551
9 R. D. Shannon: J. Appl. Phys. **73** (1993) 348. https://doi.org/10.1063/1.353856
10 R. Moolat, M. Mani, and M. Pezholil: Eng. Sci. Technol. Int. J. **32** (2022) 101063. https://doi.org/10.1016/j.jestch.2021.09.009
11 G. G. Romera, F. J. H. Martínez, M. Gil, J. J. M. Martínez, and D. S. Vargas: IEEE Sens. J. **16** (2016) 3587. https://doi.org/10.1109/JSEN.2016.2538086
12 K. Chang, I. Bahl, and V. Nair: RF and Microwave Circuit and Component Design for Wireless Systems (John Wiley & Sons, New York, 2001) 1st ed., pp. 532. https://dl.acm.org/doi/10.5555/559955
13 B. W. Hakki and P. D. Coleman: IRE Trans. Microwave Theory Tech. Conf. 8 (IEEE, 1960) 402. https://doi.org/10.1109/TMTT.1960.1124749
14 Y. Kobayashi and M. Katoh: IEEE Trans. Microwave Theory Tech. Conf. 33 (IEEE, 1985) 586. https://doi.org/10.1109/TMTT.1985.1133033
15 P. Wheless and D. Kajfez: 1985 IEEE MTT-S Int. Microwave Symp. Digest (IEEE, 1985) 473. https://doi.org/10.1109/MWSYM.1985.1132014
16 C. A. Balanis: Antenna Theory: Analysis and Design (John Wiley & Sons, New York, 1996) 2nd ed., pp. 960.
17 C. Li, X. Wei, H. Yan, and M. J. Reece: J. Eur. Ceram. Soc. **32** (2012) 4015. https://doi.org/10.1016/j.jeurceramsoc.2012.06.002
18 Y. Tohdo, K. Kakimoto, H. Ohsato, H. Yamad, and T. Okawa: J. Eur. Ceram. Soc. **26** (2006) 2039. https://doi.org/10.1016/j.jeurceramsoc.2005.09.098
19 C. Veneis, P. K. Davies, T. Negas, and S. Bell: Mater. Res. Bull. **31** (1996) 431. https://doi.org/10.1016/S0025-5408(96)00028-1
20 B. D. Silverman: Phys. Rev. **125** (1962) 1921. https://doi.org/10.1103/PhysRev.125.1921
21 W. S. Kim, T. H. Hong, E. S. Kim, and K. H. Yoon: Jpn. J. Appl. Phys. **37** (1998) 5367. https://doi.org/10.1143/JJAP.37.5367
22 K. C. Gupta, R. Garg, I. Bahl, and P. Bhartia: Microstrip Lines and Slotlines (Artech House, Boston London, 1996) 2nd ed., pp. 560.

About the Authors

Yih-Chien Chen received his B.S., M.S., and Ph.D. degrees in electrical engineering from National Cheng Kung University, Tainan, Taiwan, in 1994, 1996, and 2000, respectively. He is currently a distinguished professor in the Department of Electrical Engineering, Lunghwa University of Science and Technology, Taoyuan, Taiwan. His research interests are in microwave engineering, microwave ceramics, and sensors. (ee049@mail.lhu.edu.tw)

Tse-Lung Lin received his B.S. degree in electrical engineering from Lunghwa University of Science and Technology, Taoyuan, Taiwan, in 2021. He is currently an M.S. student in the Department of Electrical Engineering, Lunghwa University of Science and Technology, Taoyuan, Taiwan. His research interests are in microwave engineering, microwave ceramics, and sensors. (88648864a@gmail.com)